Testing for Violations of Microscopic Reversibility in ATP-Sensitive Potassium Channel Gating

Kee-Hyun Choi,† Mathew Tantama, and Stuart Licht*

Department of Chemistry, Massachusetts Institute of Technology, 77 Massachusetts Avenue, Cambridge, Massachusetts 02139

Received: December 26, 2007; Revised Manuscript Received: April 21, 2008

In pancreatic β cells, insulin secretion is tightly controlled by the cells' metabolic state via the ATP-sensitive potassium (K_{ATP}) channel. ATP is a key mediator in this signaling process, where its role as an inhibitor of K_{ATP} channels has been extensively studied. Since the channel contains an ATPase as an accessory subunit, the possibility that ATP hydrolysis mediates K_{ATP} channel opening has also been proposed. However, a rigorous test of coupling between ATP hydrolysis and channel gating has not previously been performed. In the present work, we examine whether K_{ATP} channel gating obeys detailed balance in order to determine whether ATP hydrolysis is strongly coupled to the gating of the K_{ATP} channel. Single-channel records were obtained from inside-out patches of transiently transfected HEK-293 cells. Channel activity in membrane patches with exactly one channel shows no violations of microscopic reversibility. Although K_{ATP} channel gating shows long closed times on the time scale where ATP hydrolysis takes place, the time symmetry of channel gating indicates that it is not tightly coupled to ATP hydrolysis. This lack of coupling suggests that channel gating operates close to equilibrium; although detailed balance is not expected to hold for ATP hydrolysis, it still does so in channel gating. On the basis of these results, the function of the ATPase active site in channel gating may be to sense nucleotides by differential binding of ATP and ADP, rather than to drive a thermodynamically unfavorable conformational change.

Introduction

K_{ATP} channels mediate coupling between the transmembrane electrical potential of cells and their metabolic state.[1] ADP, present in larger quantities than ATP when the cell has depleted its energy stores, stimulates channel opening, while ATP inhibits it. These channels are the first component in the signal transduction pathway leading to insulin secretion from pancreatic β cells, and they are the target of the clinically important sulfonylurea class of diabetes medications.[2]

Native K_{ATP} channels consist of two functionally distinct gene products.[3,4] One, called Kir6.2, is a potassium channel. It provides the pore for conduction of ions, switching between a "closed" nonconducting state and an "open" conducting state in a nucleotide-dependent manner and thereby mediating rapid changes in transmembrane potential. It has an ATP-binding site and a phosphatidylinositol-4,5-bisphosphate- (PIP_2-) binding site. The other, called the sulfonylurea receptor (SUR1), is homologous to the ATP-binding cassette (ABC) family of transporters, which use the free energy of hydrolysis of ATP to transport small molecules and peptides across the cell membrane.[5] SUR1 contains the binding site for sulfonylureas,[6] as well as two nucleotide binding domains (NBDs), which can bind ATP or ADP.[7,8] In this work, we investigate the possible role of ATP hydrolysis in K_{ATP} gating (i.e., the protein conformational changes that open and close the channel). Measurements of channel gating kinetics at the single-molecule level are used to determine whether channel gating exhibits the violations of microscopic reversibility expected if it is tightly coupled to ATP hydrolysis.

Several lines of evidence point to a role for ATP hydrolysis in control of K_{ATP} gating. First, MgADP binding to NBD2 of SUR1 has a stimulatory effect on channel gating.[7–9] Second, NBD2 of SUR1 hydrolyzes ATP in the presence of Mg^{2+} with a turnover number of $\sim$1.5 s^{-1} per SUR1 tetramer.[10] Finally, use of inorganic ions (orthovanadate and beryllium fluoride) to stabilize the putative prehydrolytic and posthydrolytic conformations of the cardiac channel (Kir6.2/SUR2A) shows that the prehydrolytic state favors channel closing, while the posthydrolytic state favors channel opening.[11] In suggesting that SUR1's catalytic cycle drives Kir6.2's gating conformational change, these studies raise the question of whether ATP hydrolysis is strongly coupled to the gating of the K_{ATP} channel.

However, other lines of evidence suggest that ATP hydrolysis is not tightly coupled to channel gating. The turnover number for ATP hydrolysis by NBD2 of SUR1 is much smaller than the rate constants associated with K_{ATP} channel gating.[10,12,13] This observation suggests that most Kir6.2 gating events occur independently of conformational transitions in SUR1. In addition, active site mutations in NBD2 of SUR1 expected to impair ATPase activity have modest effects on K_{ATP} gating.[13] One complicating factor in interpreting these results is the possibility that ATPase rates in the native SUR1-Kir6.2 complex are greater than those observed in the purified, detergent-solublized preparation.

In this work, we examine coupling of ATP hydrolysis to channel opening using single-channel kinetic experiments carried out on intact SUR1-Kir6.2 complexes in cell membranes. If the gating conformational change is an equilibrium process, microscopic reversibility will be obeyed, meaning that the statistical

* To whom correspondence should be addressed. E-mail: lichts@mit.edu. Telephone: 617-452-3525. Fax: 617-258-7847. Mailing address: Department of Chemistry, MIT, Room 16-573, Cambridge, MA 02139.

† Present address: Center for Chemoinformaties Research, Life Sciences Research Division, Korea Institute of Science and Technology, 39-1 Hawolgok-Dong, Seongbuk-Gu, Seoul 136–791, Korea.

10.1021/jp712088v CCC: $40.75
Published on Web 07/26/2008

properties of the single-channel record will not depend on the time direction used to measure them; that is, they are the same whether the record is "played forwards" or "played in reverse." However, if channel gating is coupled to an irreversible reaction, the characteristics of the single-channel record will not be time direction-invariant: its statistical properties will be different when it is "played in reverse." Thus, if channel gating is tightly coupled to an irreversible process such as ATP hydrolysis, the gating reaction will not exhibit microscopic reversibility.[14]

Several methods were previously used to test microscopic reversibility in single-channel experiments. One method is to obtain maximum likelihood estimates of rate constants from single-channel data either with or without the constraint of detailed balance, and compare the maximum likelihoods from each estimate.[15] If channel gating does not obey microscopic reversibility, the maximum likelihood will be greater without the detailed balance constraint than with it. A number of ion channels, including the muscle-type nicotinic acetylcholine receptor (nAChR)[16] and *N*-methyl-*D*-aspartate (NMDA) receptors (NR1-NR2A, NR2B, or NR2C),[17,18] have been analyzed using this method. The resulting likelihood ratios suggested that gating transitions between fully open states and closed states of these channels is time-reversible. A second method is to compare two-dimensional distributions of pairs of adjacent open and closed dwell-times in forward and reverse time directions; these distributions will differ if gating violates microscopic reversibility.[19] This method was used for analysis of the gating of a large conductance Ca^{2+}-activated potassium (BK) channel.[19] The difference between the two distributions was not statistically significant, consistent with the hypothesis that BK channel gating obeys microscopic reversibility. Cross-correlation functions of open and closed dwell-times were also used to test time reversibility in channel gating.[20,21] This approach was applied to single-channel records from the locust muscle glutamate receptor (GluR).[20] Cross-correlation functions in the forward/reverse time directions appeared to be identical, suggesting that GluR gating is an equilibrium process.

Only a few ion channels to date have been shown to be driven by external energy sources. The cystic fibrosis transmembrane conductance regulator (CFTR), a chloride channel, exhibits nonequilibrium gating.[22] This channel is an ATPase and a member of the ATP-binding cassette superfamily.[23] A one-dimensional dwell-time distribution analysis was used to test violations of microscopic reversibility of CFTR gating. When gating takes place at thermodynamic equilibrium, dwell-time distributions will be a sum of decaying exponential components with their maxima at $t = 0$.[24] For CFTR, however, closed time distributions for CFTR have maxima at times greater than zero; the paucity of short closed events constitutes strong evidence that an irreversible step must precede channel opening. The ATP concentration dependence of CFTR gating rate constants suggests that ATP hydrolysis is this irreversible step.[22]

For several channels, nonequilibrium transitions are observed among subconductance states (states with conductances intermediate between fully closed and fully open). This type of nonequilibrium gating is observed in the *Torpedo* ClC-0 chloride channels,[25,26] nAChRs,[27] both recombinant and native NMDA receptors (NR1-NR2D),[28–30] and mutant NMDA receptors (NR1 N598Q-NR2A).[31] Nonequilibrium transitions between subconductance states were also observed in curare-activated nAChR gating[32] and Ba^{2+}-induced BK channel gating.[33] The external energy sources for gating asymmetry are unclear in some cases. However, irreversible gating of the ClC-0 chloride channels and the NMDA receptors appeared to be driven by flow of the permeant ions down the transmembrane electrochemical gradient.[25,26,31]

Experimental Methods

Molecular Biology. Mouse pCMV-Kir6.2 and hamster pECE-SUR1 cDNA were provided by S. Seino (Chiba University, Chiba, Japan) and J. Bryan (Baylor College of Medicine, Houston, TX), respectively. A stop codon was introduced into the mouse Kir6.2 cDNA to delete the last 26 amino acids of the C-terminus (Kir6.2 ΔC1−26) using the QuikChange Site-Directed Mutagenesis Kit (Stratagene, La Jolla, CA). All cDNA constructs were verified by DNA sequencing (MIT Biopolymers Laboratory, Cambridge, MA). Plasmids were prepared for transient transfection using the QIAfilter Plasmid Maxi Kit (QIAGEN Inc., Valencia, CA).

Cell Culture. Human embryonic kidney (HEK) 293 cells (American Type Culture Collection, Manassas, VA) were cultured in Dulbecco's modified Eagle's medium containing 10% (v/v) fetal bovine serum in humidified 5% CO_2 at 37 °C. Cells were passaged every three days by treatment with trypsin.

DNA Transfection. HEK-293 cells were transiently transfected with either mouse Kir6.2 plus hamster SUR1 or Kir6.2 ΔC1−26 cDNA. pEGFP-N1 vector (BD Biosciences, San Jose, CA) was cotransfected as a marker with the cDNA of interest using the FuGENE 6 Transfection Reagent (Roche Applied Science, Indianapolis, IN). Transfection was performed according to the manufacturer's instructions with total 1 μg of cDNA per 35-mm culture dish (2:3:5 ratio of Kir6.2, SUR1, and pEGFP-N1 or 1:4 ratio of Kir6.2 ΔC1−26 and pEGFP-N1). Transfected cells were incubated in humidified 5% CO_2 at 37 °C. Approximately 36 to 72 h after transfection, the cells were used for single-channel recordings.

Electrophysiology. Micropipettes were pulled from borosilicate glass capillaries (MTW 1B150F-4; World Precision Instruments Inc., Sarasota, FL) on a puller (PP-830; Narishige Group, Tokyo, Japan) with resistance typically ∼5−12 MΩ. Pulled pipettes were coated with Sylgard (Dow Corning Corporation, Midland, MI) and fire-polished using a microforge (MF-830; Narishige Group, Tokyo, Japan) to reduce the noise level. Single-channel currents were recorded using the inside-out patch clamp configuration at a membrane potential of −80 mV, with the pipette (extracellular) solution containing (in mM): 140 KCl, 10 NaCl, 1.1 $MgCl_2$, and 10 K-HEPES, pH to 7.3 and with the bath (intracellular) solution containing (in mM): 140 KCl, 10 NaCl, 1.1 $MgCl_2$, 0.5 $CaCl_2$, 5 K-EGTA, and 10 K-HEPES, pH to 7.3.[34] 1 mM MgATP (ATP magnesium salt; Sigma, St. Louis, MO) and 5 μM PIP_2 (Calbiochem, San Diego, CA) were directly added to the bath solution.[35] Single-channel recordings were performed at room temperature with an Axopatch 200B patch clamp amplifier (Axon Instruments Inc., Union City, CA) and were low-pass filtered (10 kHz) with a 4-pole Bessel filter. Single-channel data were acquired and digitized at 20 kHz using QuB software (www.qub.buffalo.edu).[36,37]

Single-Channel Data Analysis. K_{ATP} channel recordings where only single openings but no double openings (i.e., two channels open simultaneously) were observed for 10 min were analyzed. Digitized single-channel records were filtered at 5 kHz and idealized using the half-amplitude method with the QuB software. The observed open probability (P_o) is 0.46 ± 0.09 (N = 5, S.D.) with the lowest P_o observed at 0.39. Dwell-time distributions were fitted using the maximum interval likelihood (MIL) function in the QuB software suite, which provides

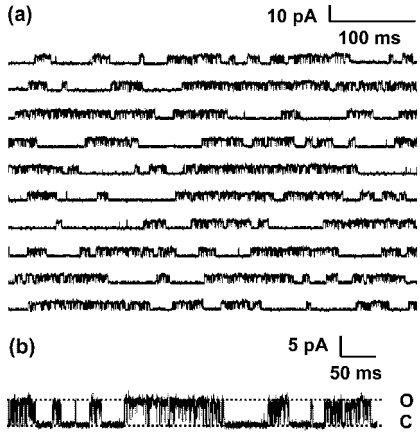

Figure 1. A representative recording of a single K_{ATP} channel in an excised inside-out patch. (a) Open probability (P_o) of K_{ATP} channel in the presence of 1 mM ATP and 5 μM PIP_2 is 0.46 ± 0.09 ($N = 5$, S.D.). (b) Expanded single-channel trace of K_{ATP} channel, showing closed and open states.

maximum likelihood estimates for rate constants in a specified model. A dead time of 0.1 ms was used for missed event correction.[24]

When n_o consecutive single openings have been observed, the probability of observing more single openings before the first multiple opening occurs is $P(r \geq n_o) = \pi^{(n_o-1)}$, where r is a total number of consecutive single openings and π is the probability that one open channel is closed before a second channel is open.[24] The probability π can be estimated as $(1 - P_o)/(1 - P_o/N)$, where N is the actual number of independent channels in the patch. An observed K_{ATP} channel record contains $\sim 2 \times 10^5$ consecutive single openings with P_o of ≥ 0.39. The probability of a run this long, $P(r \geq 2 \times 10^5)$, therefore, would be <0.0001 if there were two channels present, so it is very likely that exactly one channel is present.

Results

To test for violations of microscopic reversibility due to ATP hydrolysis, single-channel currents were recorded from inside-out membrane patches of transiently transfected HEK-293 cells in the presence of 1 mM MgATP and 5 μM PIP_2 in the bath solution (Figure 1). These conditions are expected to allow both channel opening and ATP hydrolysis.[10,38] PIP_2 has been identified as a modulator that binds to Kir6.2 subunits and adjusts the apparent inhibition constant (K_i) for ATP to within the range of cytosolic [ATP]; K_is of ATP for K_{ATP} inhibition in the absence or presence of 5 μM PIP_2 are 10.5 μM and 3.6 mM, respectively.[38,39] ATP concentration in the millimolar range is expected to support SUR1-catalyzed ATP hydrolysis since K_M for ATP hydrolysis by the purified K_{ATP} channel is 0.4 mM.[10] Membrane patches containing exactly one channel were analyzed (see Experimental Methods), and an open probability (P_o) of 0.46 ± 0.09 ($N = 5$, S.D.) was observed.

Kinetically distinct states of K_{ATP} have been observed in previous single-channel electrophysiological studies.[40–43] Binding of MgATP drives the K_{ATP} complex into a long-lived closed state. Binding of MgADP, on the other hand, drives the channel into a bursting state in which the channel rapidly opens and closes. If channel gating is tightly coupled to ATP hydrolysis, these kinetically defined states of K_{ATP}—a bursting state and an interburst closed state—might correspond to intermediates in the ATP hydrolysis cycle. Single-channel records were analyzed to determine whether transitions between the bursting and interburst states exhibit detailed balance violations.

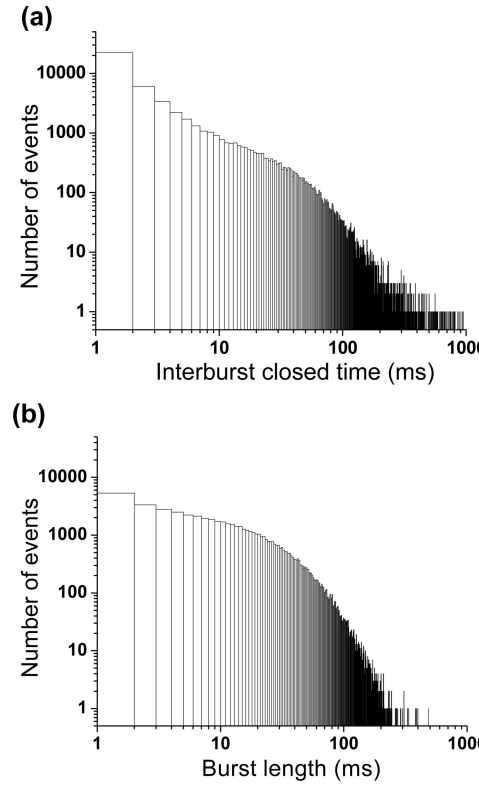

Figure 2. Dwell-time distribution analysis. Probability density function of the interburst closed time (a) and the burst length (b) distributions of K_{ATP} channels ($\sim 6.0 \times 10^4$ events with 1 ms critical time to define a burst; a bin size of 1 ms). Using smaller bin sizes down to 0.1 ms (the dead time) failed to reveal any paucity of short events in the observed exponential distributions of the dwell times.

Dwell-Time Distribution Analysis. If an irreversible step is present in K_{ATP} channel gating, the characteristic dwell time on the interburst closed state or the bursting state will be determined by the ATP hydrolysis rate at SUR1. A paucity of short events in the probability density function of the dwell-time distribution is predicted if an irreversible enzymatic step precedes channel gating, since the "hidden" enzymatic step acts to introduce a lag time into observed transitions.[24] The probability density functions of burst lengths and interburst closed dwell-times pooled from the five membrane patches (distributions were calculated for $\sim 6.0 \times 10^4$ events using a bin size of 1 ms; a critical time of 1 ms was used for assigning burst lengths[24]) were determined. These distributions were exponential, having maxima at time zero as judged by dwell-time histograms (Figure 2). The one-dimensional dwell-time distributions are therefore consistent with channel gating occurring independently of ATP hydrolysis.

Maximum Likelihood Analysis. As another test for non-equilibrium gating, correlations in time between observations of kinetically defined states were measured. Violations of microscopic reversibility would correspond to excursions through a cyclic mechanism in one direction (e.g., clockwise) occurring more frequently than excursions in the other direction (e.g., counterclockwise); in other words, detailed balance would not be obeyed. Thus, violations of microscopic reversibility in channel gating can be detected by determining whether imposing the detailed balance constraint decreases the maximum likelihood.[44] The significance of the increase in the maximum likelihood by removing the detailed balance constraint can be statistically evaluated using the likelihood ratio test. The difference between the log likelihoods (LLs) multiplied by a

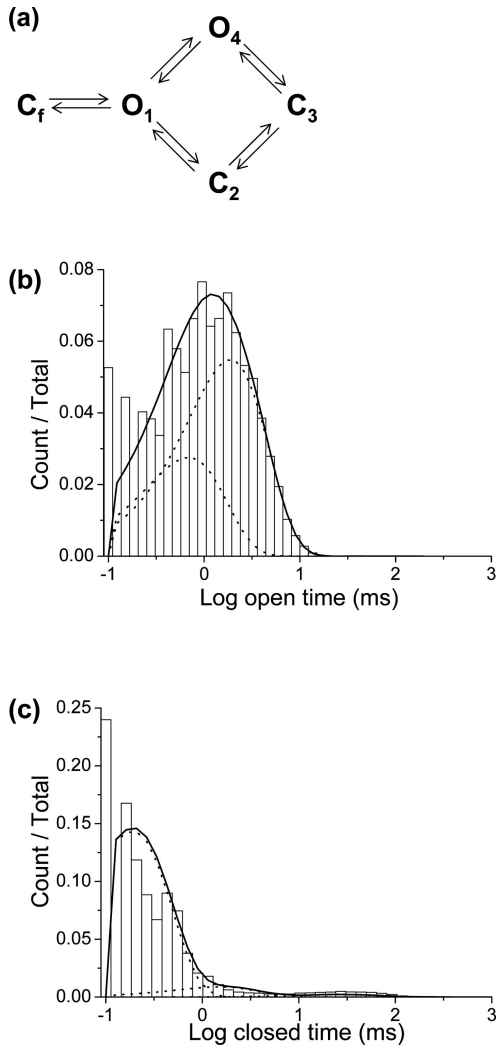

Figure 3. Maximum likelihood analysis. (a) A kinetic scheme contains the two open states (O_1 and O_4), the intraburst closed state (C_f) and the two interburst closed states (C_2 and C_3). (b) The open dwell-time histogram with the fit for a kinetic model (a) is composed of the sum (solid line) of two exponential components (dotted lines). (c) The distribution of closed times consists of the sum (solid line) of three exponential components (dotted lines). The difference in maximum log likelihoods obtained for the constrained ($O_1 \rightarrow C \rightarrow C_3 \rightarrow O_4$) and unconstrained fitting is insignificant for all five recordings (2ΔLL of $0.1 \pm 0.1 < 3.84$). Each file has $\sim 2.1 \times 10^5$ events and LL/event is 6.5 ± 0.1 ($N = 5$, S.D.) with absolute LLs of $\sim 1.3 \times 10^6$.

factor of 2 is asymptotically distributed as the χ^2 statistic. Thus, one can assess for statistical significance using χ^2 significance levels. Since detailed balance imposes one constraint, the χ^2 has 1 degree of freedom. When the 2-fold likelihood ratio (2ΔLL) is greater than 3.84, the observed increase in the maximum log likelihood is significant at the 5% level.

For maximum likelihood fitting, a kinetic scheme containing the two one open states (O_1 and O_4), the intraburst closed state (C_f) and the two interburst closed states (C_2 and C_3) was used (Figure 3a). Although more complex models have also been proposed for K_{ATP} channel gating,[41,42,45] the two-open-three-closed-states model is a minimal model that accounts for the kinetic behavior of the wild-type K_{ATP} channel in the presence of ATP and PIP_2.[34] The two open states represent PIP_2-bound and -unbound forms of the open channel, while the three closed states represent a long-lived ATP-bound form of the closed channel and two ATP-unbound closed forms. In this five-state model, the ATP-bound open state and the PIP_2-bound closed state are not included, because the binding of these metabolites biases the channel conformation strongly to the closed and open states, respectively.[1]

Since bursting kinetics is an intrinsic property of the Kir6.2 channel,[42,46] intraburst open and closing events are presumably not affected by ATP hydrolysis by SUR1. Thus, in this model, the intraburst closed state (C_f) is placed out of the cycle so that only the burst/interburst transitions are subject to the detailed balance constraint. The open and closed dwell-time distributions were fitted to the kinetic model in Figure 3a either without or with the constraint of detailed balance ($O_1 \rightarrow C_2 \rightarrow C_3 \rightarrow O_4$) (Figure 3, parts b and c). LL/event calculated from the maximum likelihood fitting of each file ($\sim 2.1 \times 10^5$ events) is 6.5 ± 0.1 ($N = 5$, S.D.) with absolute LLs of $\sim 1.3 \times 10^6$. The difference in maximum log likelihoods obtained for the constrained and unconstrained fitting is not statistically significant for any of the five recordings (2ΔL of $0.1 \pm 0.1 < 3.84$), consistent with an absence of microscopic reversibility violations.

Two-Dimensional Dwell-Time Distribution Analysis. As a further test for microscopic reversibility violations, two-dimensional (2D) dwell-time distributions were obtained from single-channel recordings in the forward and in the reverse directions in time. The 2D distributions of pairs of adjacent burst and interburst dwell-times represent the frequency of occurrence and correlation between adjacent dwell times.[47] If detailed balance is obeyed, there will be no difference between the 2D distributions in the forward/reverse time directions.[14] A χ^2 test can be performed to determine whether differences between the two distributions are significant. If the Z-score, defined as $(2\chi)^{1/2} - (2D - 1)^{1/2}$, from a χ^2 test is higher than 1.96 with more than 100 degrees of freedom (D), violations of microscopic reversibility are significant at the 5% level, i.e., microscopic reversibility is violated.[48] The 2D dwell-time distributions calculated in forward and reverse time directions from K_{ATP} single-channel recordings (>10 000 events with 1 ms critical time) are identical within experimental uncertainty (Figure 4); Z-score of 1.7 ± 0.1 ($N = 5$, S.E.M.) with >200 degrees of freedom.

Cross-Correlation Function Analysis. Cross-correlation functions have also been used to test for violations of microscopic reversibility.[20] Cross-correlation functions for kinetically distinguishable states will be nonsymmetric with respect to the sign/direction of time if microscopic reversibility is violated.[49] The dwell-time cross-correlation function is defined by $G_{oc}(k) = \mathrm{Cov}\,[O(i), C(i+k)]/(\mathrm{Var}\,[O(i)]\ \mathrm{Var}\,[C(i)])^{0.5}$, where Cov is covariance, $O(i)$ is the ith open time, $C(i)$ is the ith closed time, k is the lag (0, 1,...) and Var is variance. The same holds for cross-correlation function in the opposite time direction, defined by $G_{co}(k) = \mathrm{Cov}\,[C(i), O(i+k)]/(\mathrm{Var}\,[C(i)]\ \mathrm{Var}\,[O(i)])^{0.5}$. Non-null cross-correlation functions can be observed when the minimum (N_p) of the number of open gateway states and closed gateway states (i.e., states directly linked to a state of the opposite class, such as an open state linked to a closed state[50]) is larger than 1,[51,52] as is the case for the cyclic models considered here. At thermodynamic equilibrium, the open−closed and closed−open cross-correlations ($G_{oc}(k)$ and $G_{co}(k)$) are identical. Inequality of $G_{oc}(k)$ and $G_{co}(k)$, on the other hand, would be consistent with irreversibility in channel gating.

Open and closed dwell-times from five K_{ATP} single-channel records ($\sim 1.3 \times 10^6$ events) were pooled to generate cross-correlation functions. The cross-correlation functions revealed a weak, negative correlation between closed times and preceding and following open times up to a lag $\sim k = 10$ (Figure 5). Nonzero cross-correlations indicate multiple gateway states (N_p

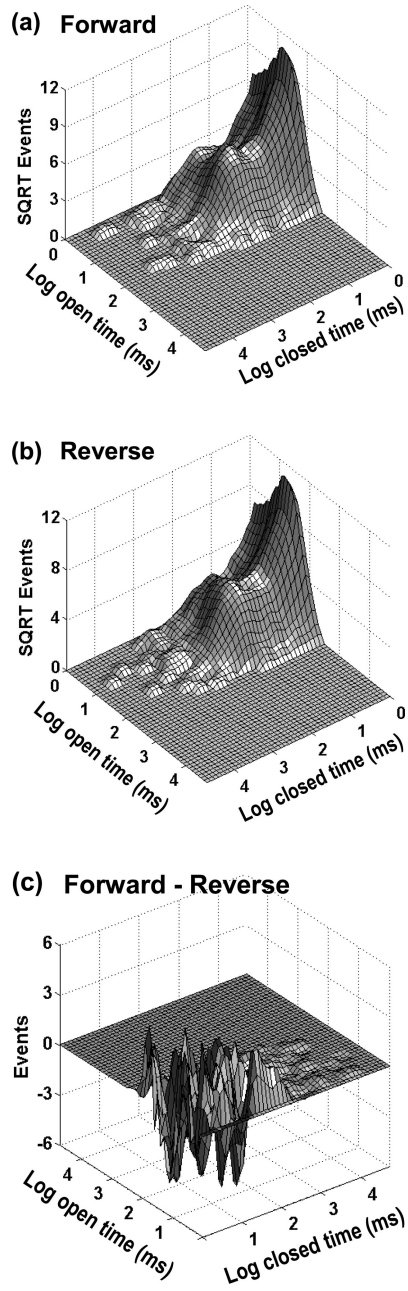

Figure 4. Two-dimensional dwell-time distribution analysis. The forward (a) and reverse (b) 2D dwell-time distributions from K_{ATP} single-channel recordings (>10 000 events with 1 ms critical time to define a burst) has no statistical differences; Z-score of 1.7 ± 0.1 (N = 5, S.E.M.) with >200 degrees of freedom. (c) Difference between the forward and reverse dwell-time distributions is not statistically significant; less than five events in each bin.

> 1) in the underlying mechanism of the K_{ATP} channel gating. The negative correlation indicates that the long closed state is linked to the relatively short open state.[16] These observations are consistent with the previously proposed kinetic mechanism of K_{ATP} channel gating.[34,45] There was no significant difference between $G_{oc}(k)$ and $G_{co}(k)$ obtained from K_{ATP} single-channel data (Figure 5). The cross-correlation analysis is therefore consistent with gating of K_{ATP} occurring as an equilibrium process.

Detection Limit of Each Method. Because no significant violations of microscopic reversibility were detected using any of the tests employed, it is important to establish lower limits for the magnitude of detailed balance violations detectable by these methods. To examine what extent of irreversibility is detectable by each method, single-channel data were first simulated with the best fit model for the observed K_{ATP} channel recordings (Figure 3a) with the same record length as the experimental records (10 min) using the following rate constants (s^{-1}): $k_{21} = 100$, $k_{23} = 100$, $k_{32} = 100$, $k_{43} = 100$, $k_{41} = 100$, $k_{14} = 100$, $k_{15} = 5000$, and $k_{51} = 5000$. Single-channel data with detailed balance violations of varying magnitude were generated by varying k_{12} and k_{34}. The magnitude of detailed balance violations can be quantified by calculating the asymmetry in the transition frequencies, which can be expressed by $(f_{AB} - f_{BA})/(f_{AB} + f_{BA})$ when the transition frequency f_{AB} from state A to state B is given by the product of the equilibrium occupancy p_A times the rate constant for the transition k_{AB}.[53] The equilibrium state occupancies were calculated using the Q-matrix method.[54]

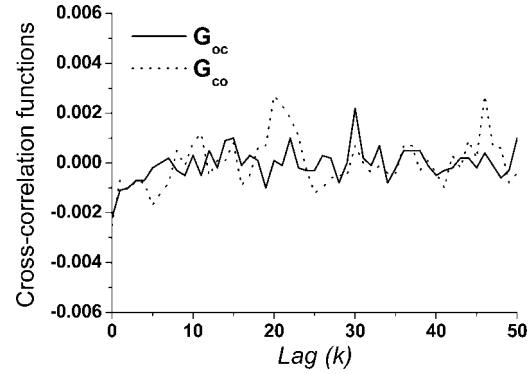

Figure 5. Cross-correlation function analysis. Cross-correlation functions (solid line for $G_{oc}(k)$ and dotted line for $G_{co}(k)$) derived from K_{ATP} single-channel recordings (~1.3×10^6 events from five different membrane patches) show a weak, negative cross-correlation.

A 2.7% violation of detailed balance (k_{12} and k_{34} = 90 s^{-1}) was not detectable using any of the methods; 2ΔLL of 3.1 (<3.84) and Z-score of 0.7 (<1.96). When the detailed balance violation was increased to 4.2% (k_{12} and k_{34} = 85 s^{-1}), it was detectable by the maximum likelihood analysis but not by the 2D dwell-time distribution analysis; 2ΔLL of 16.7 and Z-score of 0.7. Finally, a detailed balance violation of 5.9% (k_{12} and k_{34} = 80 s^{-1}) was detected both by the 2D dwell-time distribution analysis and the maximum likelihood analysis; 2ΔLL of 15.0 and Z-score of 2.9.

ATP-Independent Violations of Microscopic Reversibility on Time Scales Longer than Burst/Interburst Transitions. K_{ATP} also appears to undergo changes in activity on time scales longer than those associated with the predominant transition between bursting and nonbursting states. As previously observed,[41,46,55] the closed time distribution for K_{ATP} exhibits a number of closed components longer than the predominant interburst interval of ~10 ms. Qualitatively, large shifts in average channel activity are observable on the time scale of seconds and above (Figure 6a).

To determine whether the slow changes in average channel activity obey microscopic reversibility, third-order correlation functions, defined as $G_2(\tau_1, \tau_2) = \langle A(0)A(\tau_1)A(\tau_1 + \tau_2)\rangle$,[49] were calculated for records in which activity $A(t)$ was averaged over 100 ms (Figure 6b). For thermodynamically reversible processes, the third-order correlation function is symmetric with respect to the sign/direction of time, and equal to its transpose when expressed as a matrix. The difference between the third-order correlation function and its transpose ($G_2 - G_2^T$) therefore provides a way to measure violations of microscopic reversibility.

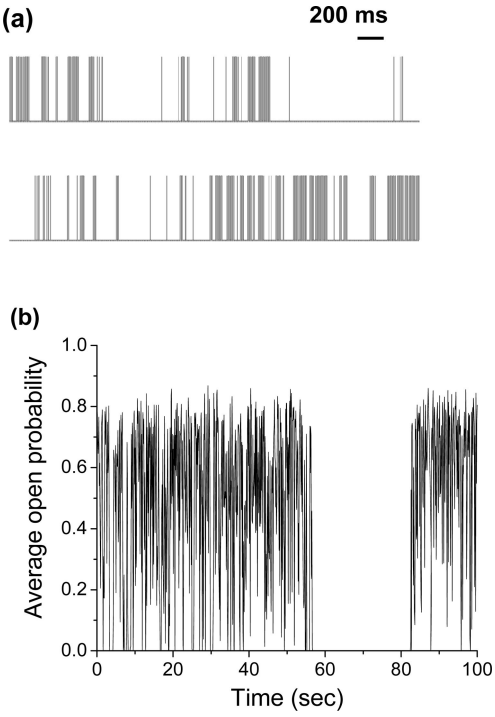

Figure 6. K_{ATP} undergoes changes in activity on longer time scales. (a) Channel activity changes substantially on the time scale of seconds and above; channel activity is shown as a record of idealized channel openings. (b) Channel activity (open probability, P_o) averaged over 100 ms.

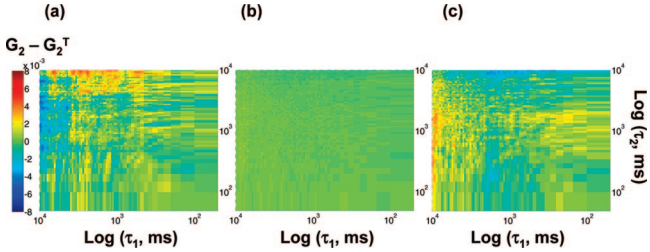

Figure 7. Third-order correlation functions. (a) The observed maximum relative asymmetry for average K_{ATP} activity was 0.015 ± 0.002 of $G_2 - G_2^T$. (b) Channel activity for a mutant Kir6.2 channel in the absence of SUR1 exhibits a symmetric third-order correlation function ($G_2 - G_2^T = 0.003 \pm 0.001$). (c) Recordings obtained from K_{ATP} channels in the absence of ATP exhibit asymmetric third-order correlation functions ($G_2 - G_2^T = 0.012 \pm 0.002$).

Third-order correlation functions for average K_{ATP} activity are not symmetric, consistent with violations of microscopic reversibility (Figure 7a). The experimentally observed maximum relative asymmetry ($G_2 - G_2^T = 0.015 \pm 0.002$; $N = 7$, S.E.M.) is comparable to that observed in simulated records of comparable length in which detailed balance is violated ($G_2 - G_2^T = 0.01 \pm 0.001$; $N = 5$, S.E.M.) (Supporting Figure S3a). In the simulated data, asymmetry in the third-order correlation functions is apparent at time scales >1 s, as expected from the mechanism used, in which transitions through the cycle occur on the time scale of seconds. Asymmetry in the experimental data is pronounced only on time scales >1 s as well, indicating that if it is associated with bursting/nonbursting transitions, it can only be associated with the slowest of these transitions. For both simulated and experimental data, decay in the third-order correlation function is evident on time scales >1 s (Supporting Figure S1), indicating that the observed asymmetry is not simply due to random fluctuations in uncorrelated channel activity.

The SUR1 subunit is necessary for violations of microscopic reversibility to occur. Channel activity for a mutant Kir6.2 channel that can be expressed in the absence of SUR1[56] exhibits a symmetric third-order correlation function (Figure 7b) ($G_2 - G_2^T = 0.003 \pm 0.001$; $N = 5$, S.E.M., comparable to simulated records for a gating reaction at equilibrium where $G_2 - G_2^T = 0.006 \pm 0.001$; $N = 5$, S.E.M.; Supporting Figure S3b). However, ATP is not required for violations of microscopic reversibility to be observed (Figure 7c). Recordings obtained in the absence of bath-applied ATP exhibit asymmetric third-order correlation functions ($G_2 - G_2^T = 0.012 \pm 0.002$; $N = 6$, S.E.M.), indistinguishable from those observed in the presence of ATP. These observations indicate that slow conformational changes of K_{ATP} are coupled to an irreversible process other than ATP hydrolysis.

Discussion

Lack of Evidence for Violations of Detailed Balance in the Dominant Mode of K_{ATP} Channel Gating. The four dwell-time-based analyses used to test for deviations from microscopic reversibility provide no evidence for such deviations. Each method, however, has a limit on the magnitude of microscopic reversibility violations that it can detect. For records of the length used in this study, 2D dwell-time distribution analysis has the detection limit of ~6% irreversible opening and closing transitions. One could detect up to ~4% irreversible gating using the maximum likelihood analysis. Thus, even if there is a small excess of flux through one direction of a gating cycle, it is less than ~4−6% of the total gating transitions.

In addition to the detection limit on the magnitude of detailed balance violations, there are unique issues of interpretation associated with each of the analyses. The maximum likelihood analysis is most sensitive in detecting violations and statistically straightforward because the log likelihood ratio distribution follows a χ^2 distribution.[44] However, unlike the other analyses, the maximum likelihood analysis is model-dependent, since it assumes a specific gating mechanism. Unambiguous assignment of detailed gating mechanisms is generally difficult since multiple mechanisms often provide comparably good fits to the data when the underlying kinetics is complex. In addition, the maximum likelihood analysis is performed based on the aggregated Markov models where the estimation of the transition rates is burdened by the issue of the nonidentifiability in certain models.[44] If transition rates from two formally distinct states are equal, dwell times arising from those states may not be experimentally identifiable as arising from separate states, lowering the power to detect violations of microscopic reversibility. Dwell-time distribution analysis is limited by uncertainties associated with finite record length. These uncertainties are greatest in the tails of histograms, i.e., the longer time scales, where bins have the lowest counts. Long recordings are thus required to minimize these uncertainties. Finally, cross-correlation function analysis is more general and easy to carry out. However, cross-correlation functions may also be of insufficient magnitude to be interpreted for time reversibility. Omission of short dwell-times (bursting events) due to the finite bandwidth of records may decrease the apparent magnitude of correlations,[20] as would be the case if there is a correlation between the occurrence of long closed dwells and short open dwells. Also, when the rates of the open-open and closed-closed transitions are fast compared to the rates of open-closing transitions, the degree of cross-correlation could be reduced.[20]

Time-Asymmetric Slow Activity Changes That Do Not Require ATP Hydrolysis. Although analyses of the relatively fast (1−100 ms) gating conformational changes of K_{ATP} provide

no evidence for violations of microscopic reversibility, slower changes in activity do violate microscopic reversibility as determined by the observation of time-asymmetric third-order correlation functions. However, it is important to note that a slow decrease in channel open probability ("rundown") is often observed in K_{ATP} channels, particularly in the absence of PIP_2.[57] Slow incorporation of PIP_2 into the membrane, which would cause a slow increase in channel open probability, might also occur. Slow decreases or increases in open probability (i.e., nonstationary records) could manifest themselves as apparent violations of microscopic reversibility. To investigate this possibility, a test for stationarity of channel activity was performed by calculating the linear trend in channel activity (averaged over 10 ms). Channel activity of wild-type and mutant channels changes globally at a rate of 5×10^{-4} and 7×10^{-4} channel openings/s (0.2−0.3% of the mean activity per second), respectively. The global trends are comparable for the mutant, which exhibits negligible asymmetry in its third-order correlation function, and the wild-type, which exhibits measurable asymmetry; global trends in channel activity therefore appear not to account for the observed asymmetry in the third-order correlation function.

As for the dwell-time-based methods described above, third-order correlation functions will fail to detect microscopic reversibility violations if the mechanism does not have a sufficient number of identifiable states. In previous work,[21,49] it has been noted that ion channel systems often fail to meet this criterion because the open and closed states are the only states of distinguishable conductance. However, states that are identifiable kinetically rather than through conductance also produce time asymmetric third-order correlation functions (an example is provided in the Supporting Information). For K_{ATP}, the multiple nonbursting states (observed as multiple kinetic components in the closed time distribution) are likely to be the kinetically identifiable states that allow time-asymmetric third-order correlation functions to be observed.

Coupling to some irreversible processes appears to require the presence of the SUR1 subunit since the recordings of the Kir6.2 subunit alone exhibit time-symmetric third-order correlation functions. However, the deviations from microscopic reversibility are independent of the presence of ATP. The lack of ATP dependence supports the conclusion that ATP hydrolysis by SUR1 is not directly coupled to conformational changes of Kir6.2. However, the observation of SUR1-dependent time-asymmetric behavior suggests that K_{ATP} gating is coupled to some other irreversible processes. One potential candidate is PIP_2 hydrolysis. PIP_2 is present in HEK-293 membranes, and phospholipase C (the enzyme that hydrolyzes PIP_2) may be retained in membrane patches since it is membrane-associated.[58] Modulation of K_{ATP} activity coupled to ongoing PIP_2 hydrolysis might account for the violations of microscopic reversibility observed on the time scale of seconds. If PIP_2 is depleted slowly over the course of the experimental record, but individual hydrolysis events take place on the time scale of seconds, microscopic reversibility violations might be observed due to local depletion of PIP_2 without being accompanied by substantial macroscopic rundown. Slow PIP_2-dependent rundown (on the time scale of hours at submicromolar Ca^{2+}) has been reported previously for K_{ATP};[57] at the higher calcium concentrations used in the current experiments, this process might still be sufficiently slow to account for the observed microscopic reversibility violations without causing large decreases in open probability. Previous studies indicate that the C-terminal truncation affects channel trafficking without affecting channel gating;[56] differences between mutant and wild-type channels are thus not likely to be due to the lack of the C-terminus in the mutant. Allosteric interactions between SUR1 and phospholipase C might facilitate PIP_2 hydrolysis by phospholipase C, which may account for SUR1-depedent nonequilibrium processes. Further studies will be required to resolve these issues.

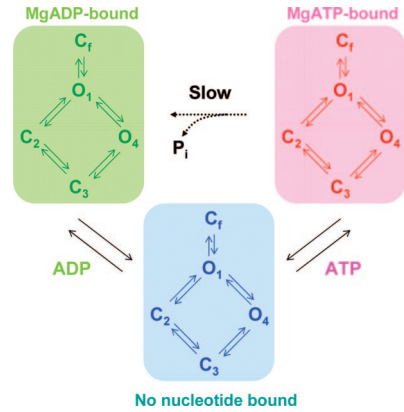

Figure 8. Proposed allosteric mechanism. Direct transitions between MgATP-bound and MgADP-bound states via ATP hydrolysis would be rare compared to indirect transitions via dissociation of one nucleotide and binding of the other nucleotide. Nucleotides would therefore act like allosteric inhibitors/activators of channel activity.

Implications for the Physiological Role of the SUR1 ATPase Active Site. The lack of observed microscopic reversibility violations associated with ATP hydrolysis suggests that the physiological role of SUR1 is not to couple ATP hydrolysis to gating of Kir6.2. However, previous work has clearly shown that binding of nucleotides to the SUR1 NBDs affects channel activity.[7–9] One possibility that accommodates all of the kinetic data is that ATP hydrolysis is much slower than channel gating in the intact, native channel. In that case, MgATP and MgADP would act much like classical allosteric inhibitors/activators of channel activity. Binding of MgATP or MgADP to the SUR1 NBDs would shift the conformational equilibrium to the nonbursting and bursting conformations, respectively. However, direct transitions between MgATP-bound and MgADP-bound states via ATP hydrolysis would be rare compared to indirect transitions via dissociation of one nucleotide and binding of the other nucleotide (Figure 8). In this mechanism, the NBDs can be thought of as sensing relative nucleotide concentration through equilibrium binding rather than as motors driving a cycle of gating conformational changes.

Conclusions

Coupling of the K_{ATP} channel gating reaction to the thermodynamically irreversible ATP hydrolysis reaction has been proposed. Using single-channel kinetics, the microscopic reversibility of gating reactions was quantitatively characterized to address the question of whether K_{ATP} carries out nonequilibrium gating. Based on consistent results from several independent analyses, the dominant mode of channel gating does not violate microscopic reversibility, implying that ATP hydrolysis is not directly coupled to channel gating. Signatures of irreversibility are observed at longer time scales, but these are not associated with ATP hydrolysis. Thus, SUR1 might act as a sensor of ATP/ADP ratio in the presence of saturating ATP physiologically, rather than act as a motor to drive the gating conformational change.

Acknowledgment. We thank Profs. Susumu Seino, Joseph Bryan, and Lydia Aguilar-Bryan for providing plasmids,

Shaunna Stanton for preparing a mutant channel construct, and Prof. Jianshu Cao and Dr. James Witkoskie for helpful discussions. The authors declare no conflict of interest.

Supporting Information Available: Text detailing the mechanisim of the simulations, analysis, and kinetics and figures showing the third-order correlation function of experimental records, cyclic mechanisim of channels, third-order correlation functions, kinetic identifiability in detection, kinetically identifiable bursting states, and a kinetically non-identifiable and non-equilibrium cyclic mechanism. This material is available free of charge via the Internet at http://pubs.acs.org.

References and Notes

(1) Nichols, C. G. *Nature* **2006**, *440*, 470.
(2) Ashcroft, F. M. *J. Clin. Invest.* **2005**, *115*, 2047.
(3) Seino, S.; Miki, T. *Prog. Biophys. Mol. Biol.* **2003**, *81*, 133.
(4) Ashcroft, F. M.; Gribble, F. M. *Trends Neurosci* **1998**, *21*, 288.
(5) Jones, P. M.; George, A. M. *Eur. J. Biochem.* **2000**, *267*, 5298.
(6) Aguilar-Bryan, L.; Nichols, C. G.; Wechsler, S. W.; Clement, J. P.; Boyd, A. E.; Gonzalez, G.; Herrera.Sosa, H.; Nguy, K.; Bryan, J.; Nelson, D. A. *Science* **1995**, *268*, 423.
(7) Gribble, F. M.; Tucker, S. J.; Ashcroft, F. M. *EMBO J.* **1997**, *16*, 1145.
(8) Nichols, C. G.; Shyng, S. L.; Nestorowicz, A.; Glaser, B.; Clement, J. P. t.; Gonzalez, G.; Aguilar.Bryan, L.; Permutt, M. A.; Bryan, J. *Science* **1996**, *272*, 1785.
(9) Shyng, S.; Ferrigni, T.; Nichols, C. G. *J. Gen. Physiol.* **1997**, *110*, 643.
(10) Mikhailov, M. V.; Campbell, J. D.; de.Wet, H.; Shimomura, K.; Zadek, B.; Collins, R. F.; Sansom, M. S. P.; Ford, R. C.; Ashcroft, F. M. *EMBO J.* **2005**, *24*, 4166.
(11) Zingman, L. V.; Alekseev, A. E.; Bienengraeber, M.; Hodgson, D.; Karger, A. B.; Dzeja, P. P.; Terzic, A. *Neuron* **2001**, *31*, 233.
(12) Masia, R.; Enkvetchakul, D.; Nichols, C. G. *J. Mol. Cell Cardiol.* **2005**, *39*, 491.
(13) Bienengraeber, M.; Alekseev, A. E.; Abraham, M. R.; Carrasco, A. J.; Moreau, C.; Vivaudou, M.; Dzeja, P. P.; Terzic, A. *FASEB J.* **2000**, *14*, 1943.
(14) Rothberg, B. S.; Magleby, K. L. *Biophys. J.* **2001**, *80*, 3025.
(15) Wagner, M.; Timmer, J. *J. Theor. Biol.* **2001**, *208*, 439.
(16) Colquhoun, D.; Sakmann, B. *J. Physiol.* **1985**, *369*, 501.
(17) Gibb, A. J.; Colquhoun, D. *J. Physiol.* **1992**, *456*, 143.
(18) Stern, P.; Behe, P.; Schoepfer, R.; Colquhoun, D. *Proc. Biol. Sci.* **1992**, *250*, 271.
(19) Song, L.; Magleby, K. L. *Biophys. J.* **1994**, *67*, 91.
(20) Ball, F. G.; Kerry, C. J.; Ramsey, R. L.; Sansom, M. S. P.; Usherwood, P. N. R. *Biophys. J.* **1988**, *54*, 309.
(21) Steinberg, I. Z. *Biophys. J.* **1986**, *50*, 171.
(22) Zeltwanger, S.; Wang, F.; Wang, G. T.; Gillis, K. D.; Hwang, T. C. *J. Gen. Physiol* **1999**, *113*, 541.
(23) Riordan, J. R.; Rommens, J. M.; Kerem, B.; Alon, N.; Rozmahel, R.; Grzelczak, Z.; Zielenski, J.; Lok, S.; Plavsic, N.; Chou, J. L.; et al. *Science* **1989**, *245*, 1066.
(24) Colquhoun, D.; Hawkes, A. G. The principles of the stochastic interpretation of ion-channel mechanisms. In *Single-channel recording*, 2nd ed.; Sakmann, B., Neher, E., Eds.; Plenum Press: New York, NY, 1995; pp 397.
(25) Chen, T. Y.; Miller, C. *J. Gen. Physiol.* **1996**, *108*, 237.
(26) Richard, E. A.; Miller, C. *Science* **1990**, *247*, 1208.
(27) Hamill, O. P.; Sakmann, B. *Nature* **1981**, *294*, 462.
(28) Wyllie, D. J. A.; Behe, P.; Nassar, M.; Schoepfer, R.; Colquhoun, D. *Proc. R. Soc. London B: Biol. Sci.* **1996**, *263*, 1079.
(29) Momiyama, A.; Feldmeyer, D.; Cull.Candy, S. G. *J. Physiol.* **1996**, *494*, 479.
(30) Cull-Candy, S. G.; Usowicz, M. M. *Nature* **1987**, *325*, 525.
(31) Schneggenburger, R.; Ascher, P. *Neuron* **1997**, *18*, 167.
(32) Trautmann, A. *Nature* **1982**, *298*, 272.
(33) Bello, R. A.; Magleby, K. L. *J. Gen. Physiol.* **1998**, *111*, 343.
(34) Ribalet, B.; John, S. A.; Xie, L. H.; Weiss, J. N. *J. Physiol.* **2006**, *571*, 303.
(35) Lin, Y. W.; Jia, T.; Weinsoft, A. M.; Shyng, S. L. *J. Gen. Physiol.* **2003**, *122*, 225.
(36) Qin, F.; Auerbach, A.; Sachs, F. *Proc. R. Soc. London B: Biol. Sci.* **1997**, *264*, 375.
(37) Qin, F.; Auerbach, A.; Sachs, F. *Biophys. J.* **2000**, *79*, 1915.
(38) Shyng, S. L.; Nichols, C. G. *Science* **1998**, *282*, 1138.
(39) Baukrowitz, T.; Schulte, U.; Oliver, D.; Herlitze, S.; Krauter, T.; Tucker, S. J.; Ruppersberg, J. P.; Fakler, B. *Science* **1998**, *282*, 1141.
(40) Enkvetchakul, D.; Loussouarn, G.; Makhina, E.; Nichols, C. G. *Biophys. J.* **2001**, *80*, 719.
(41) Enkvetchakul, D.; Loussouarn, G.; Makhina, E.; Shyng, S. L.; Nichols, C. G. *Biophys. J.* **2000**, *78*, 2334.
(42) Li, L.; Geng, X.; Drain, P. *J. Gen. Physiol.* **2002**, *119*, 105.
(43) Trapp, S.; Proks, P.; Tucker, S. J.; Ashcroft, F. M. *J. Gen. Physiol.* **1998**, *112*, 333.
(44) Wagner, M.; Timmer, J. *Biophys. J.* **2000**, *79*, 2918.
(45) Enkvetchakul, D.; Nichols, C. G. *J. Gen. Physiol.* **2003**, *122*, 471.
(46) Proks, P.; Capener, C. E.; Jones, P.; Ashcroft, F. M. *J. Gen. Physiol.* **2001**, *118*, 341.
(47) Rothberg, B. S.; Magleby, K. L. *Methods Enzymol.* **1998**, *293*, 437.
(48) Snedecor, G. W.; Cochran, W. G. *Statistical methods*; Iowa State University Press: Ames, IA, 1989; Vol. 76; p 468.
(49) Qian, H.; Elson, E. L. *Proc Natl Acad Sci U S A* **2004**, *101*, 2828.
(50) Fredkin, D. R.; Montal, M.; A., R. J. Identification of aggregated Markovian models: application to the nicotinic acetylcholine receptor. In *Proceedings of the Berkeley Conference in Honor of Jerzy Neyman and Jack Kiefer*; Le Cam, L. M., Olshen, R. A., Eds.; Wadsworth Press: Monterey, CA, 1985; Vol. 1; pp269.
(51) Ball, F. G.; Sansom, M. S. *Biophys. J.* **1988**, *53*, 819.
(52) Colquhoun, D.; Hawkes, A. G. *Proc. R. Soc. London B: Biol. Sci.* **1987**, *230*, 15.
(53) Lauger, P. Conformational transitions of ionic channels. In *Single-channel recording*, 2nd ed.; Sakmann, B., Neher, E., Eds.; Plenum Press: New York, NY, 1995; p 651.
(54) Colquhoun, D.; Hawkes, A. G. A Q.matrix cookbook. In *Single-channel recording*, 2nd ed.; Sakmann, B., Neher, E., Eds.; Plenum Press: New York, NY, 1995; p 589.
(55) Drain, P.; Li, L.; Wang, J. *Proc Natl Acad Sci U.S.A.* **1998**, *95*, 13953.
(56) Tucker, S. J.; Gribble, F. M.; Zhao, C.; Trapp, S.; Ashcroft, F. M. *Nature* **1997**, *387*, 179.
(57) Ribalet, B.; John, S. A.; Weiss, J. N. *J. Gen. Physiol.* **2000**, *116*, 391.
(58) Singer, W. D.; Brown, H. A.; Sternweis, P. C. *Annu. Rev. Biochem.* **1997**, *66*, 475.

JP712088V